On the potential for an inversion of the permafrost active layer: the impact of seawater on permafrost degradation in a coastal zone imaged by electrical resistivity tomography (Hornsund, SW Spitsbergen)

Marek Kasprzak[1], Mateusz C. Strzelecki[1], Marta Kondracka[2], Andrzej Traczyk[1], Michael Lim[3], Krzysztof Migała[1]

[1] University of Wrocław, Institute of Geography and Regional Development, pl. Uniwersytecki 1, 50-137 Wrocław, Poland,

[2] University of Silesia, Faculty of Earth Sciences, ul. Będzińska 60, 42-700 Sosnowiec, Poland

[3] Northumbria University, Engineering & Environment, Wynn Jones Building 201, Northumberland Road, Newcastle upon Tyne NE1 8ST, UK

Abstract

This paper presents the results of two-dimensional electrical resistivity tomography (ERT) of permafrost developed in coastal zone of Hornsund, SW Spitsbergen. Using the ERT inversion results, we studied the 'sea influence' on deeper parts of the frozen ground. The study builds on previous ground temperature measurements conducted in several boreholes located in study area, which captured the propagation of ground heat waves from the base of permafrost. Our resistivity models indicate a major differentiation in terms of resistivity of permafrost in the coastal zone. The resistivity measures obtained reveal exceptionally low resistivity in deepest layers of permafrost at the coast and continuing further inland. We interpret this inversion as the result of seawater temperature and salinity influences affecting the basal layers of permafrost. Based on repeat ERT surveys, two years apart, we detect significant changes in the distribution of resistivity, within both the surface and basal active layers, dependent on the thermal, physical and chemical characteristics of seawater. Finally, strong morphological control is seen into govern the spatial patterns of behavior within the surface and basal active layers and potentially influence coastal susceptibility to storm events.

keywords: coastal permafrost, active layer, electrical resistivity tomography (ERT), Spitsbergen, Arctic

Correspodence:

Marek Kasprzak, marek.kasprzak@uni.wroc.pl ; Matt Strzelecki: mat.strzelecki@gmail.com

Introduction

Surprisingly, only a few observations to date exist regarding the role of permafrost on High Arctic coastal evolution (e.g. McCann and Hannell 1971). In many High Arctic fjords, coastal permafrost is relatively young, having developed after deglaciation and isostatic sea-level fall, and is often divided by taliks. Consequently, the influence of permafrost on coastal development is less clear than along the ice-rich permafrost coasts of Siberia and Alaska where older permafrost has controlled coastal evolution for several hundred thousand years (Wetterich et al. 2008; Schirrmeister et al. 2010; Kienast et al. 2011, Overduin et al. 2014). Nevertheless, permafrost and permafrost-related processes may affect polar beach sediment budgets and is the second most important agent in modification of micro-relief, after sea-ice (Trenhaile 1997). The presence of permafrost is effective in protecting beach sediments from erosion. Cox and Monde (1985) calculated that under the same wave conditions, frozen gravel berms erode up to 10 times more slowly than an unfrozen gravel berm. The spatial distribution of coastal permafrost and its transition to submarine permafrost under the High Arctic fjords seafloor is largely unexplored, although several studies exist that detail the thermal state of the beach and intertidal zone. For instance, McCann and Hannell (1971) monitored development of the active layer across the High Arctic intertidal zone in Cornwallis and Devon Islands. Between 1967–69, they observed that in several profiles the depth of the active layer increased slowly toward the low water mark, but it was not significantly deeper than the active layer above high water mark.

Despite over a century of permafrost research in Spitsbergen, the thickness, type (continuous, discontinuous) and thermal state of coastal permafrost have not been sufficiently studied. One of the first permafrost depth calculations in Spitsbergen was conducted by Werner Werenskiold (1922) who calculated that in front of flat coastal zones (tidal flats, barrier coasts), permafrost should reach 100 m below sea level. Werenskiold (1922) suggested that in case of fjord systems, only in those with widths exceeding 400 m would have had conditions enabling thawing of the fjord bottom. More recent calculations concerning the permafrost thickness and detailed field surveys have helped geothermal gradients – about 2–2.5°C/100 m in central Spitsbergen (e.g. Liestøl 1976, Péwé 1979; Humlum et al. 2003). Instrument data on the thermal state and thickness of Spitsbergen permafrost has been obtained from ground temperature measurements in deep boreholes (Oberman and Kakunov 1978, Isaksen et al. 2001, Harris et al. 2009, Christiansen et al. 2010). However, to our knowledge, the majority of boreholes used in permafrost monitoring studies in Svalbard are located inland (in valley and slope systems) and hence do not record changes in thermal state of intertidal zone or submarine slopes. In general, the permafrost thickness in Spitsbergen is stated to be from less than 100 m in the coastal zone up to 500 m in highlands (Humlum *et al*. 2003). In this paper we adopt the definition of coastal permafrost presented by Gregresen and Eidsmoen (1988) during their pilot study of the thermal state of shoreface in Svea and Longyearbyen as a 'warm permafrost', developing within a transition zone between frozen and unfrozen ground. Data on Spitsbergen's coastal permafrost has been provided by measurements of ground electrical resistivity conducted by Harada and Yoshikawa (1996, 1988) who specified that the permafrost thickness under delta deposits in Adventfjorden is closer to 30 m. Important advances to permafrost base investigations have also been provided by research on subpermafrost groundwater systems (e.g. Haldorsen et al. 1996, Booij et al. 1998, Haldorsen et al. 2010, Ploeg et al. 2012).

Difficulties with drilling through permafrost are likely to have limited the attention of researchers mainly to the permafrost active layer. Over last 50 years numerous investigations of active layer development and thermal state have been carried out in western and central Spitsbergen i.e. Baranowski (1968); Jahn (1982); Grześ (1985); Migała (1994); Leszkiewicz and Caputa (2004); Christiansen and Humlum (2008); Rachlewicz and Szczuciński (2008); Westermann et al. (2011); Dolnicki et al. (2013); and Byun et al. (2014). It has also been suggested that increasing permafrost degradation associated with marine processes may be expected, primarily along coastal lowlands, with rising temperatures (Etzelmüller et al. 2011).

Sea influences on permafrost

Previous studies on the thermal state of permafrost in the vicinity of the Polish Polar Station in Hornsund by Alfred Jahn (1982) and year-round measurements (31 July 1986 – 29 June 1987) conducted by Krzysztof Migała (Chmal et al. 1988) have highlighted the importance of sea influence on spatial distribution. Temperature measurements in a 3 m deep borehole (Fig. 1) identified the occurrence of episodic heat waves in the winter. The appearance of heat waves was thought to be associated with the landward propagation of heat from the sea or the thermal state (warm) of underground waters. However, evidence supporting such hypotheses has not been provided. It is worth noting that observations described by Chmal et al. (1988) are not isolated. Similar phenomena in the area of Hornsund have been described by Baranowski (1968). In a 1.6 m deep borehole, he noticed an increase of ground temperature at the end of May 1958, demonstrating some heat supply from the bottom. Baranowski (1968) explained the fact with the seepage of seawaters through a loose structure of marine terrace non longer protected by shore ice and pancake ice. In the beginning of May 1958 the average temperature of the coastal waters was 0.35°C, and was slightly higher than the ground temperature, and by 2.2°C higher than the air temperature at the altitude of 2 m above the ground. The temperature difference measured between the fjord water temperature (up to 2.9°C) and the temperature of deeper ground sections (on the level –1.6 m) was 5°C.

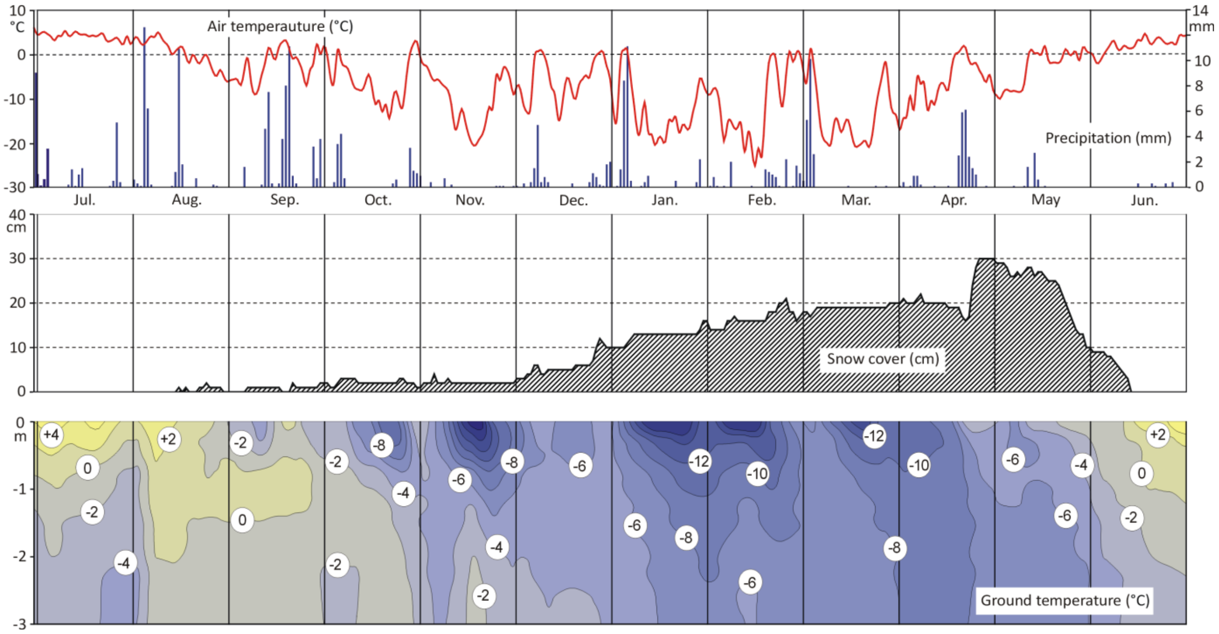

Fig. 1. Ground temperature changes in 3 m borehole drilled in the vicinity of the Polish Polar Station in Hornsund during winter 1986–1987 (after Chmal et al. 1988, modified).

Since Baranowski's study (1968) the concept of 'reversed' active layer induced by landward heat wave from warmer sea water has never been sufficiently tested and clarified. Therefore the purpose of this pilot study was to determine if the proximity of sea affects thermal state and spatial distribution of permafrost using geophysical methods. The scheme of our investigations is presented in Figure 2.

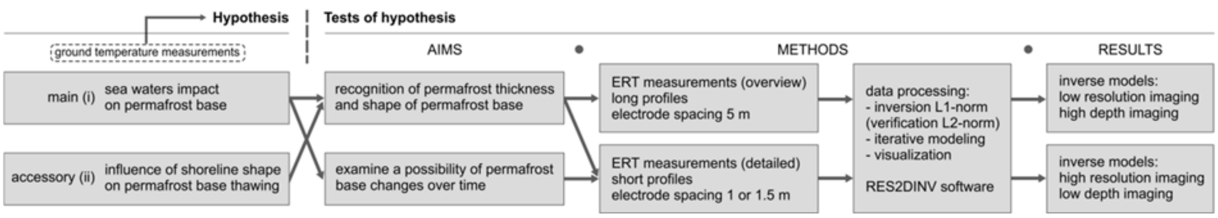

Fig. 2. The scientific plan of ERT investigations of coastal permafrost in Hornsund.

We started our search for ‘coastal impact’ on permafrost during pilot electrical resistivity tomography (ERT) measurements conducted across coastal zones of Hyttevika and Steinvika, small rocky bays located along northern coast of Hornsund. The results of pilot survey from summer 2012 proved a potential usefulness of the ERT method in detection both the thickness of permafrost in the coastal zone and shape of permafrost base. Analysis of pilot results led to determination of two research hypotheses:

(i) the impact of seawater (temperature, salinity) may cause one-year changes in the shape of the (coastal) permafrost base similar to those observed in active layer;

(ii) the impact of seawater on inland permafrost depends on the coastal zone shape (stronger influence on the shape of permafrost body in headlands exposed to the open sea than in embayments).

To test our hypotheses we run the second measurement campaign in summer 2014, when in addition to profiles in Hyttevika and Steinvika the measurements were conducted in a third bay – Veslebogen. We understand that the ERT results, however relatively suggestive, do not provide direct evidence of permafrost base thawing, such as ground temperature monitoring (Dobiński 2011). Nevertheless, based on the experience of other authors using the ERT in permafrost research (see references in *Methods*) we believe that the method is very helpful in determining the permafrost base shape in the coastal zone.

Methods

Electrical resistivity tomography (ERT) is one of the near-surface geophysics which is commonly utilised in non-invasive ground investigation (e.g. Samouëlian et al., 2005, Schrott and Sass, 2008, Van Dam, 2012, Loke *et al.* 2013). ERT is frequently applied in projects focusing on detection of permafrost and various forms of ground ice (e.g. MacKay 1969, King and Seppälä 1987, Seguin et al. 1988, Hauck 2002, Ishikawa 2004, Yoshikawa et al. 2006, Krautblatter and Hauck 2007, Kneisel *et al*., 2008, Harris *et al.* 2009, Hilbich *et al.* 2009, Kneisel, 2010, Lewkowicz *et al.* 2011, Watanabe *et al.* 2012, Hauck 2013, You et al. 2013, Kneisel *et al.* 2014).

The essence of ERT are resistivity measurements (*R*) in several four-electrode meter circuits where an electrical current (*I*) is passed into the ground through two electrodes (C_1, C_2), and the voltage – potential difference (*V*) is measured across a second pair of electrodes (P_1, P_2). As the rock mass is not a homogeneous body, measured resistivity, expressed in the relation of the voltage to the current with factor (*k*) dependent on the electrode array and distances between the electrodes, is an apparent resistivity. Shifting the measurement sequences along the profile and enlarging the distances between the electrodes enable achieving many measuring points located in separate horizons. For achieving both a good vertical resolution and depth penetration the Wenner-Schlumberger electrode array was used (Loke 2000, Milsom 2003, Reynolds 2011). In order to conduct geophysical measurements the ARES equipment was utilised (GF Instruments, Brno, Czech Republic).

The field measurements were carried out in summer seasons 2012 (5th –8th August) and 2014 (15th – 29th of July). Surveys were made across modern gravel-dominated beaches and raised marine terraces. Each of the seven profiles was led perpendicularly to the coastline and started from the water edge. The measurements were made during the low tide in order to detect spatial distribution of coastal permafrost in the intertidal zone. The ERT profiles were divided into the lower resolution ones, but longer and deeper reaching (Profiles S1, H1, V1, V2, electrodes spacing 5 m), and profiles with higher resolution, detailing the longer profiles parts (Profiles S2, S3, H2, electrodes spacing 1 or 1.5 m). During measurements in 2012, 5 sections of active multi-electrode cables were at disposal, allowing for simultaneous connection of 40 electrodes. In 2014, 8 cable sections with 64 terminals were used simultaneously. Long profiles with smaller distance between the electrodes were achieved by application of the *roll-on* technique, which allows continuation of measurement with multiple transmission of the initial section of cables connecting the electrodes to the end of the profile. Profile V1 was run across coastal zone in an embayment (Veslebogen) and profile V2 across headland (between Veslebogen and Ariebukta) in order to check the strength of the coastline shape factor on the coastal impact on permafrost. Profiles S2 and S3 in Steinvika were led along the same profile line repeated in two-year intervals to test potential changes in the permafrost base.

The results of electrical resistivity of the base (expressed in Ω m) were subjected to standard geophysical interpretation (inversion) in the RES2DINV software (Geotomo, Malaysia). The default smoothness-constrained inversion formulation was used by the RES2DINV (last squares inversion). Measuring points with undoubtedly wrong values were eliminated from the data received. Errors were related to physical problems with the operation of the equipment in the field and weak contact of some electrodes with the base (Manual for RES2DINV 2013). The default smoothness-constrained inversion formula was used (least squares inversion, initial Damping factor = 0.160, minimum Damping factor = 0.015). Resulting models of this L1-norm inversion scheme were compared with the models achieved from the L2-norm (robust) inversion method, because the robust method reduced the effects of “outlier” data points where the noise comes from errors or equipment problems (Loke 2013). Another analysed issue was the distribution of the percentage difference between the logarithms of the observed and calculated apparent resistivity values and the points with large errors were removed (above 100 percent in root mean square error statistics).

Iterative modelling techniques produce electrical tomograms of the geological strata. Logarithmic contour intervals were used for graphic visualization of these inversion results. To enable a direct visual comparison of the values of three topography results, they were matched using a homogenous colour scale. The colour scale was constructed in a way that warm colours represent low resistivity rates (unfrozen ground), and cold colours represent high resistivity rates (frozen ground). Inversion models included information concerning the land surface topography. A distorted finite-element grid was used (distortion damping factor 0.75), where an effect of the topography is reduced with depth (Loke 2013).The geological and geomorphological interpretation of inversion results was based on the terrain mapping of landforms and sediments covering coastal plain and analysis of geological map (Czerny et al. 1992) ground-truthed by observations of rock exposures in modern and uplifted cliffs. According to the referential values of electrical resistivity of rock formations presented in selected literature (Stenzel and Szymanko 1973, Telford et al. 1990, Kearey et al. 2002, Milsom 2003, Kneisel and Hauck 2008, Reynolds 2011) it was assumed that high values of apparent resistivity ($\rho \geq 1$ kΩ m) are typical for cryotic formations. Figure 3 shows that value ranges for particular rock formations are wide and often overlap one another. Therefore the final result of our interpretation was influenced by hard to separate factors i.a. structure and texture of investigated rocks, their mineralogical composition, thickness, water content or salinity.

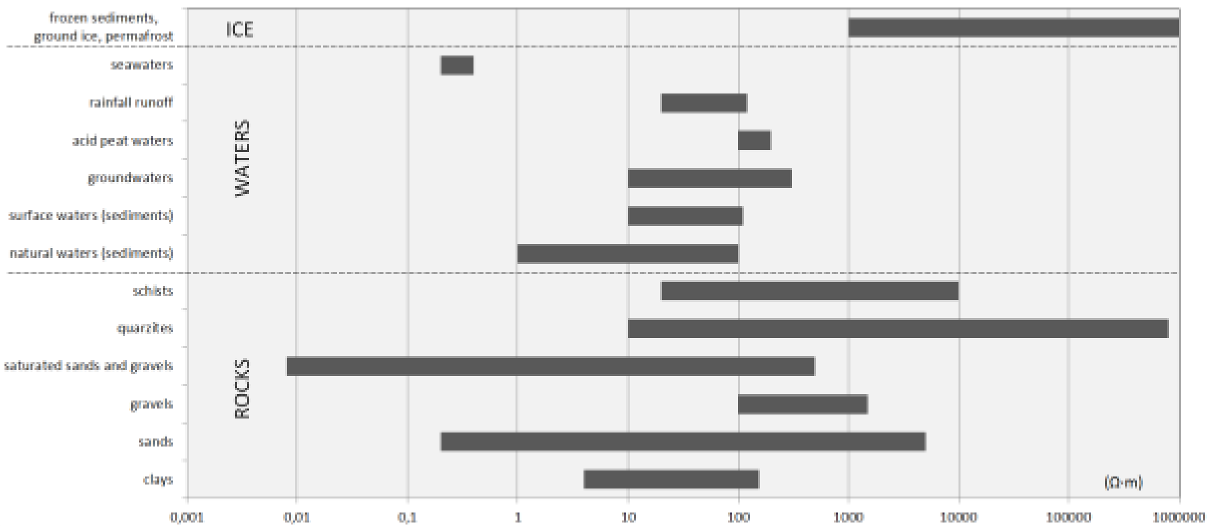

Fig. 3. Range of resistivity detected in various environments, based on: Stenzel and Szymanko (1973), Telford et al. (1990), Kearey et al. (2002), Milsom (2003), Kneisel and Hauck (2008), Reynolds (2011).

Study area

The study is located in the northern coast of Hornsund in south-western Spitsbergen (Fig.4). The coastal zone is generally low and the present-day cliffs are abraded in strandflat surface elevated by 8–25 m a.s.l. Majority of rocky cliffs are less than 10 m high. Numerous skerry islands and rocky stacks are scattered along the coast, indicating the extent of shore platform up to ca. 300 m seawards. Small embayments and coves are filled with gravel-dominated beaches which are often terminated by low cliffs. Coastal landscape is dominated by uplifted marine terraces and palaeo-skerries and rocky cliffs. Staircase of ca. 15 uplifted marine terraces reaching up to 220 m a.s.l. has been identified in the area (Jahn 1959, 1968, Chmal 1987, Karczewski et al. 1990, Migoń 1997, Zwoliński et al. 2013).

The north-western Hornsund region is underlain by Precambrian basement rocks, which are a part of lower and middle Hecla Hoek succession, covered by Cambrian and Ordovician sedimentary successions (Czerny et al. 1992). Present-day cliffs, stacks, skerries and shore platforms are formed in quartzites, schists, paragneisses, marbles and amphibolites. Due to a diverse geological structure of the coastline, the measuring points were deliberately located on fragments with lithologically homogenous bedrock. The ERT Profiles 'S' and 'H' by Sæterdalsneset (Fig. 4) were created in the area made of white and green quartzites belonging to the Gulliksenfjellet Formation, while the ERT profiles 'V' made by Veslebogen were in the reach of the Ariekammen Formation; yellow and white calcite marbles (Profile V1) and garnet-calcite-mica schists (Profile V2).

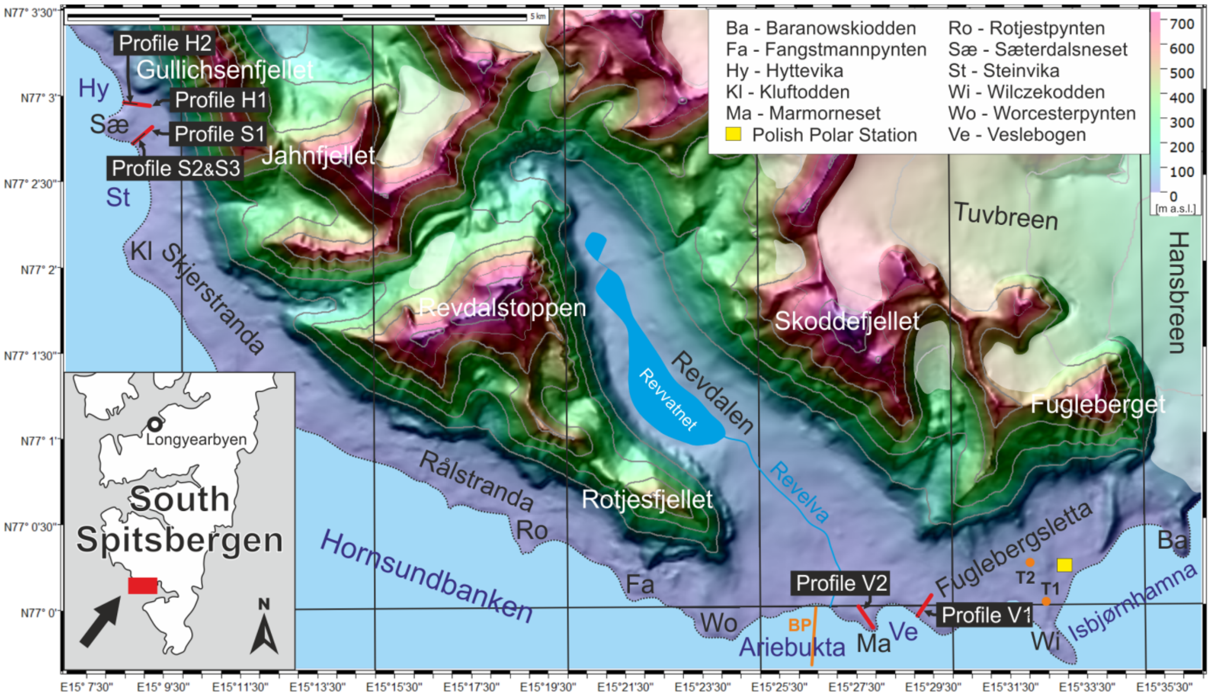

Fig. 4. Study area near Hornsund with location of electrical imaging profiling (Profiles H, S, V); BP – bathymetric profile by Swerpel (1982) showed on fig. 7, T1 – 1.6 m depth bore hole with ground temperature measurements done in 1957–1960 (Baranowski 1968), T2 – 3 m depth bore hole with ground temperature measurements done in 1986–1967 (Baranowski 1968). DEM image based on Norsk Polar Institute data.

Solid rocks of the base in the measuring points are covered with a marine sediment which are well grinded gravels and fine-grained material (Fig. 5a–d). The surface sediment cover has got a relatively little thickness, reaching maximum 2–2.5 m, which may be observed by the sea cliff bluffs (Fig. 5d). Near the paleoskerries diversifying the surfaces of raised marine terraces, the thickness of loose formations decreases. The initial pedogenesis has already transformed surface of older marine terraces (Kabała and Zapart 2009, Szymański *et al.* 2013, Migała *et al.* 2014).

Climatic conditions in northern Hornsund are common for the western Spitsbergen. The mean annual air temperature for the period of 1979–2012 was –4.1°C, with the minimum in January (–11.3°C) and maximum in July (4.4°C) (Kępski et al. 2013). The trend of annual air temperature rise for the period 1979–2009 is +0.096 (± 0.021)°C/year (Marsz 2013a). The air humidity in the area of Hornsund is significant and its average is 79.4%, increasing during the summer months (Marsz 2013b). The mean measured total precipitation for the investigated period was 434.4 mm a year, with its maximum in August (64.4 mm) (Łupikasza 2013). On average, the ground surface in Hornsund is covered with snow for 244 days a year (Niedźwiedź and Styszyńska 2013).

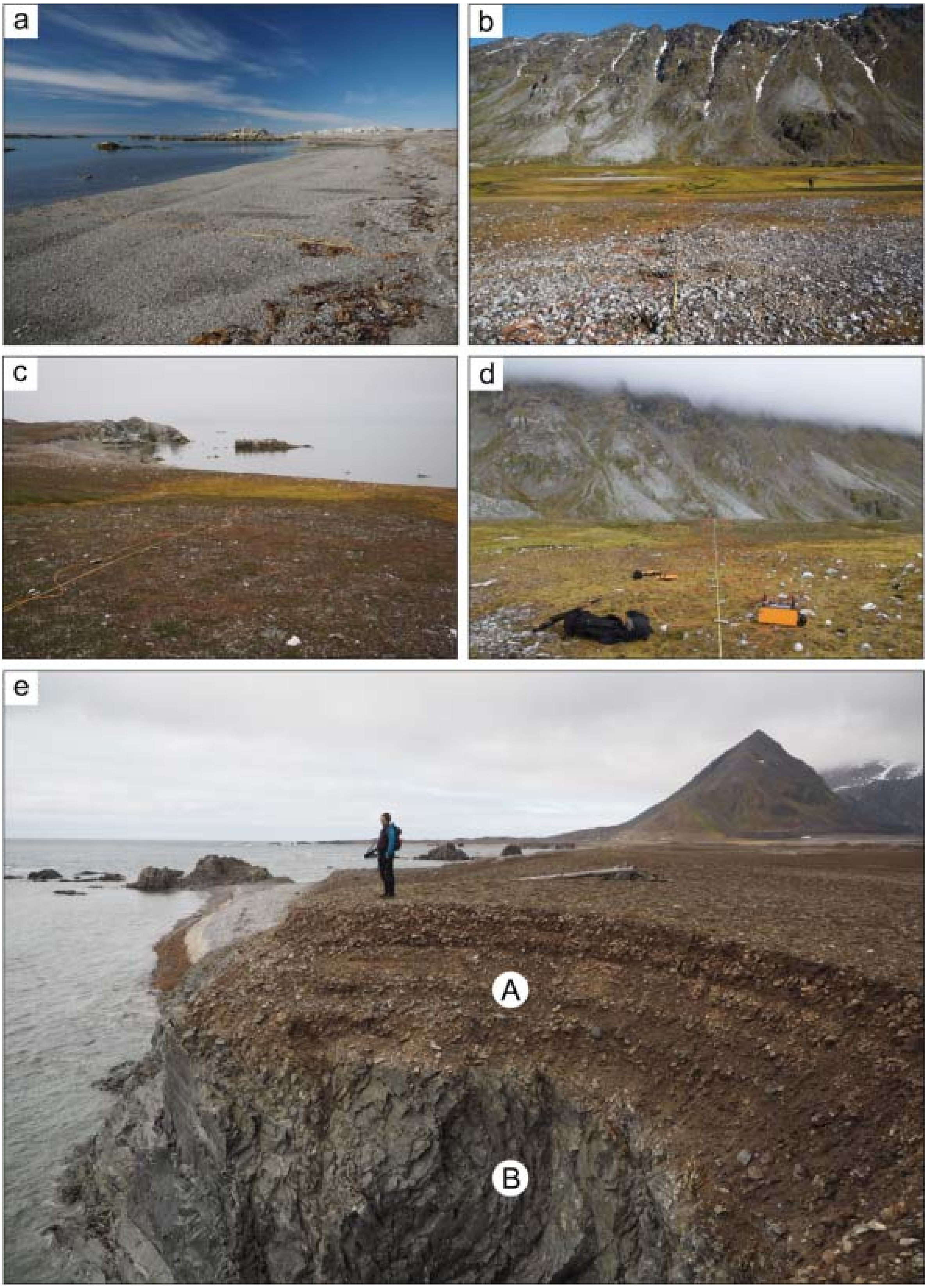

Fig. 5. Study sites selected for ERT measurements (phots by M. Kasprzak): a,b) seaward and landward views at ERT profiles in Steinvika – Profiles S1–S3; c,d) seaward and landward views at ERT profiles in Hyttevika – Profiles H1, H2; e) Headland in Veslebogen (Profiles V1, V2), A – solid rock, B – marine deposits cover.

The thickness of active layer is controlled by topography and bedrock lithology. Mean thickness of active layer is 1–1.15 m (Baranowski 1968, Jahn 1982, Grześ 1985, Migała 1994). On the raised marine terraces active layer developing in saturated clays covered by tundra reaches up to 0.7 m whereas in shallow humid depressions filled with mud active layer thaws up to 0.9 m. Active layer depth under large polygons and stone rings is 1.4 m. It thaws even deeper in uplifted beaches composed of mixed sand-gravel deposits 1.38–2.21 m (Migała 1994) and 2.30 m (Chmal et al. 1988). The thinnest active layer depths are observed in areas covered by peat (on average 0.4 m, Jahn 1982). The thawing of active layer is accelerated due to increasing high maximum temperatures. The maximum air temperature measured in the study area at the ground surface covered by tundra was 22°C (Migała *et al.* 2014). The measurements carried out other parts of Svalbard showed that extreme near-surface temperatures may cause thermal responses even up to 15 m deep (Isaksen et al. 2007). Figure 6 summarises the meteorological conditions during spring and summer periods before the measurements.

Changes of thermal conditions of water masses at the mouth of Hornsund are associated with the mixing of cold Arctic water mass carried by the East Spitsbergen Current and warm Atlantic water mass carried by the West Spitsbergen Current (Majewski et al. 2009). There is only few data on physical and chemical properties of coastal waters in the study area.

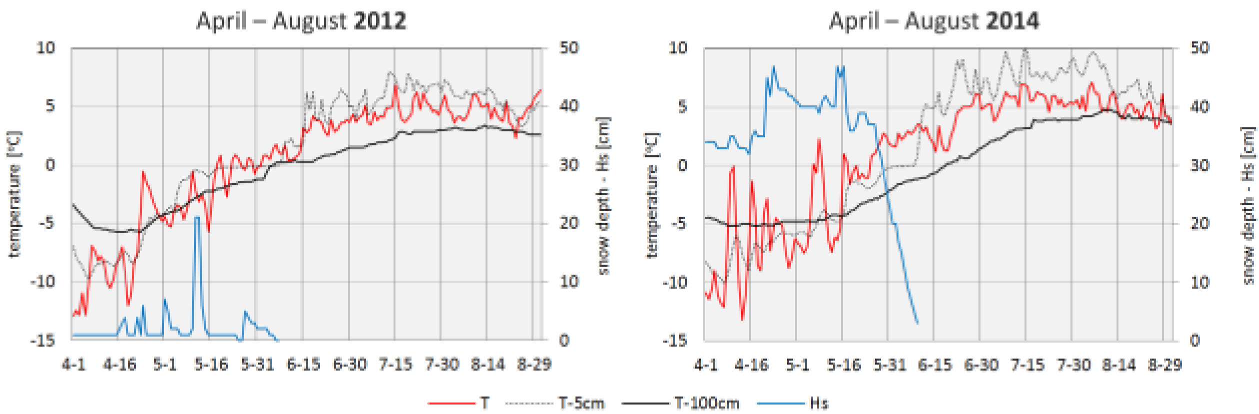

Fig. 6. Meteorological conditions before ERT measurements carried out in summers 2012 and 2014 in Hornsund: T – mean daily air temperature, T–5cm – temperature of ground at 0.05 m under the surface, T–100cm – temperature of ground 1 m under surface, H_S – snow depth. Source: Hornsund GLACIO-TOPOCLIM Database: http://www.glacio-topoclim.org (retrieved on 24th November 2014).

The bathymetric profile with measurements of water temperature and salinity was made in the summer 1975 for Ariebukta by Swerpel (1982, 1985). His study showed that the water temperature at the surface decreased from the coast towards the sea (Fig.7). At depths below 5 m a cold current was observed (water temperature below 1.4°C). In the test section salinity also grew with distance from the shore and with depth. It was the highest 33.46 ‰ at the depth of 10 m on the slope of shore platform and the lowest 14.27 ‰ by the shore of the bay. Changes of water properties were also influenced by the flux of freshwater from the Revelva, which flows into Ariebukta. At the time of measurement the mean salinity of coastal waters in Ariebukta (northen Hornsund) was 31.64‰ (Swerpel 1982). More recent study on Hornsund seawater properties was conducted by Zajączkowski et al. (2010). In the summers of 1999, 2000 and 2002, at the entrance of the Hornsund the near-bottom temperature (at 151 m depth) was 1.27–2.02 ° C and a near-bottom salinity in the summer of 2002 was 34.73 ‰. The maximum sea ice thickness in inner part of Hornsund varies is ca. 1.5 m (Gerland and Hall 2006). With favourable weather conditions, a vast coastal ice and icefoot is formed, which protects the shore from storm waves over autumn and winter months (Rodzik and Wiktorowicz 1995). The entrance to the fjord is normally ice free by the beginning of June (Urbański et al. 1980, Węsławski et al. 1988).

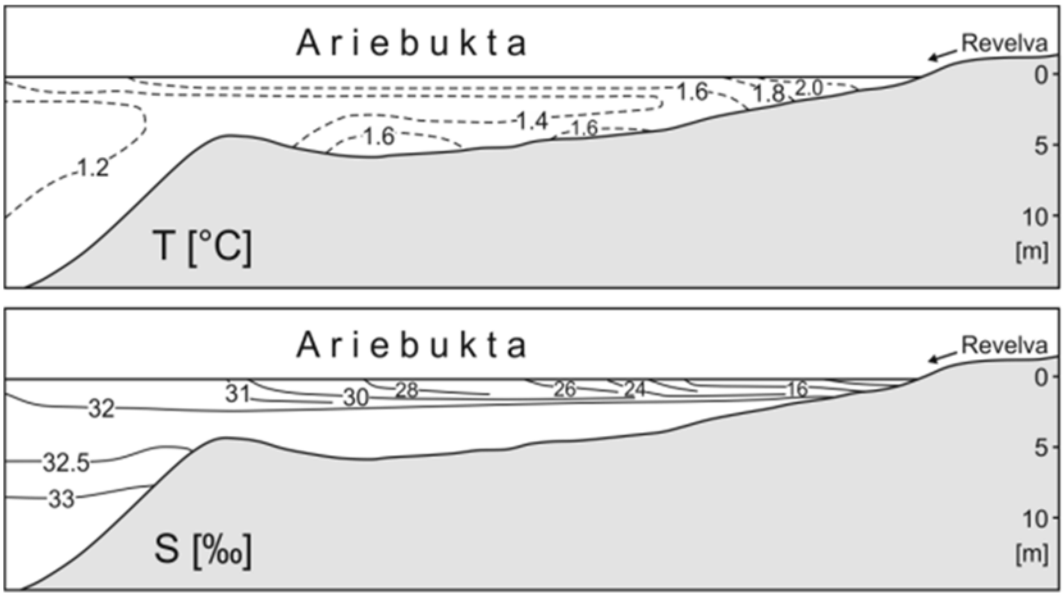

Fig. 7. Vertical water temperature (T) and salinity distribution (S) in bathymetric profile (app. 1 km long) in summer of 1975 (20th August), local sea water conditions are modified by Revelva's mounth and fresh waters inflow (after Swerpel 1982, modified)

Results and interpretation

Field investigations resulted in obtaining several inversion results showing apparent resistivity of the ground in seven measurement profiles (3 profiles in Steinvika, 2 profiles in Hyttevika, 2 profiles in Veslebogen). Table 1 summarises basic data on the measurement profiles and the results of ERT measurements. The received maximum apparent resistivity values are relatively high and are ρ_{max} 7 774.1–17 868.1 Ω m (see Fig. 3 for comparison). The median values equalled ρ_{me} 497.1–3809.0 Ω m. Large standard deviations were also registered ρ_{SD}1093.1–2941.7 Ω m, indicating a diversity of the examined rocks in terms of geoelectrical properties. 315 m long profiles based on 5 m electrode spacing allowed to penetrate the ground to the depth of ca. 50 m. Shorter profiles (71 m, 142.5 m) with the electrode spacing 1 and 1.5 m respectively reached ca.. 8 and 11–17 m depths.

Tab. 1. Summary of ERT measurements and inversion results. SD – standard deviation, RMS error – root-mean-square deviation (differences between value predicted by a model and the values measured).

No	Locality	Date	Profile length [m]	Electrode spacing [m]	Electrode array	Apparent resistivity [Ohm m]				Inversion	
						ρ median	ρ mean	ρ SD	ρ max	Iteration	RMS error
S1	Steinvika (Skjerstranda)	2014-07-15	315.0	5.0	Wenner-Schlumberger	2352.5	3327.5	2527.3	11911.2	3	5.0
S2		2014-07-15	142.5	1.5		1952.9	2115.6	1286.0	7774.1	5	3.8
S3		2012-08-08				1617.7	1785.9	1093.1	8016.0	5	5.8
H1	Hyttevika	2014-07-17	315.0	5.0		3809.0	4563.9	2651.5	10868.7	5	2.8
H2		2012-08-05	71.0	1.0		2334.1	2396.6	1265.3	5280.4	5	1.7
V1	Veslebogen (bay)	2014-07-25	315.0	5.0		6859.7	6883.1	2941.7	17868.1	5	2.6
V2	Veslebogen (headland)	2014-07-29	315.0	5.0		497.1	1165.0	1402.1	11372.6	5	7.8

Steinvika. The Steinvika case study is presented in a first place because in our opinion the results obtained from ERT measurements present a model situation of the development of 'reverse' active layer in coastal permafrost. The general state of frozen ground conditions were examined in the ERT Profile S1 extending from the coastline for 315 m inland to the foot of the massif Gullichsenfjellet (fig. 8a). The profile led from the shoreline through three marine terraces covered with well-preserved beach ridges. Except for the modern coastal zone and crests of beach ridges, the profile surface was covered with tundra. Majority of hollows and flat surfaces located ca. 60 m from the shoreline were vegetated by wet mires.

The inversion results showed that ground resistivity in close vicinity of the sea is low, which excludes the existence of permafrost, including submarine permafrost. The highest resistivity ρ > 2 kΩ m characterised the subsurface ground layer and started at ca. 20 m from the coastline, continuing inland. The tomogram points with the highest resistivity formed a wedge with thickness decreasing seawards.

Approximately 100 m off the shoreline the body of the highest resistivity had a mean thickness of up to 10 m, and up to 20 m ca. 220 m away from the sea. The surface part of the body had lower resistivity and was associated with thawed active layer. The lower boundary of the high-resistivity field had an irregular shape and was limited by points (areas) of low resistivity. The smallest resistivity was found in the intertidal zone, exposed during the low tide. The zone of low resistivity developed further inland under the frozen layer (under permafrost).

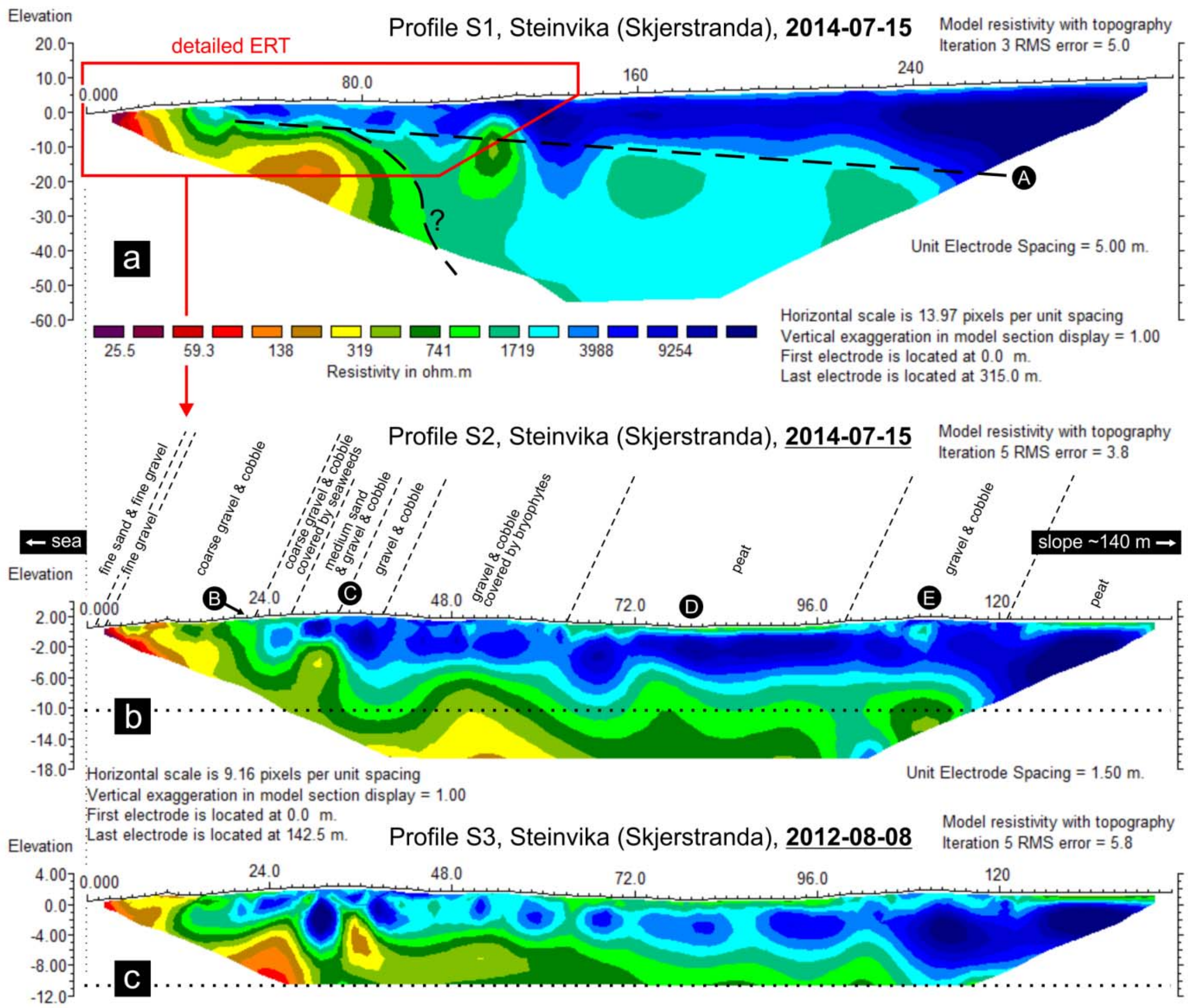

Fig. 8. a) Inversion results of electrical imaging of Profile S1 in Steinvika; b,c) detailed ERT image of coastal zone repeated in 2 years time interval (b and c). Legend: A –boundaries between permafrost and non-frozen ground below (permafrost base), B – current storm ridge and line of drift wood, C – older storm ridge, D – the lowest point between older storm ridges, E – old storm ridge. The dotted line indicates max depth of Profile 3. The colour scale was unified for all resistivity models.

First ERT measurements in Stenivika were carried out in August 2012 when 142.5 m long profile (Profile S3) with 1.5 m electrode spacing was made (fig. 8c). In July 2014 the ERT measurements were repeated following the same profile line and electrode spacing, but using a larger number of cables (fig. 8b), thus the inversion results at the same spacing between the electrodes vary in the probing depths. Smaller electrode spacing enabled obtaining a higher resolution image and helped in precise detection of active layer that formed a clearly visible layer from ca. 60 m of the profile.

The permafrost represented by points (fields) with the highest resistivity was not homogenous. In terms of geoelectrical features the fragmentation of the permafrost layer was particularly visible on Profile S3 and generally increased seawards. It is important to note that in tomogram developed from Profile S3 (August 2012) a zone of particularly high resistivity developed under the modern storm ridge (ca. 34 m of the profile), which was not observed 2 years later (profile S2). Comparison of the two detailed measurements enabled to detect temporal change in geoelectrical features of the permafrost layer, changes in the active layer thickness and changes of permafrost base with the highest resistivity.

Hyttevika. In contrast to Steinvika site the ERT profile (Profile H1) carried out across Hyttevika coastal zone (fig. 9a) was characterised by steeper slope. The inversion results allowed to distinguish the body with the highest resistivity reaching the coastal zone and underlying zone of lower resistivity developing inland from the sea. A narrow (ca. 5 m wide) coastal strip by the shoreline exposed during a low tide was characterised by low resistivity excluding presence of permafrost. Until the 180 m of the ERT profile the thickness of the body with the highest resistivity did not exceed 15 m.

The interpretation of the lower parts of the tomogram was more difficult. This is due to the interpolation effects caused by extremely different values of single points occurring at the edges of the tomogram. The system of geoelectrical features in the centre part of the profile suggested, however, the existence of a boundary between thawed and frozen parts of the coastal zone at 180 m of the profile.

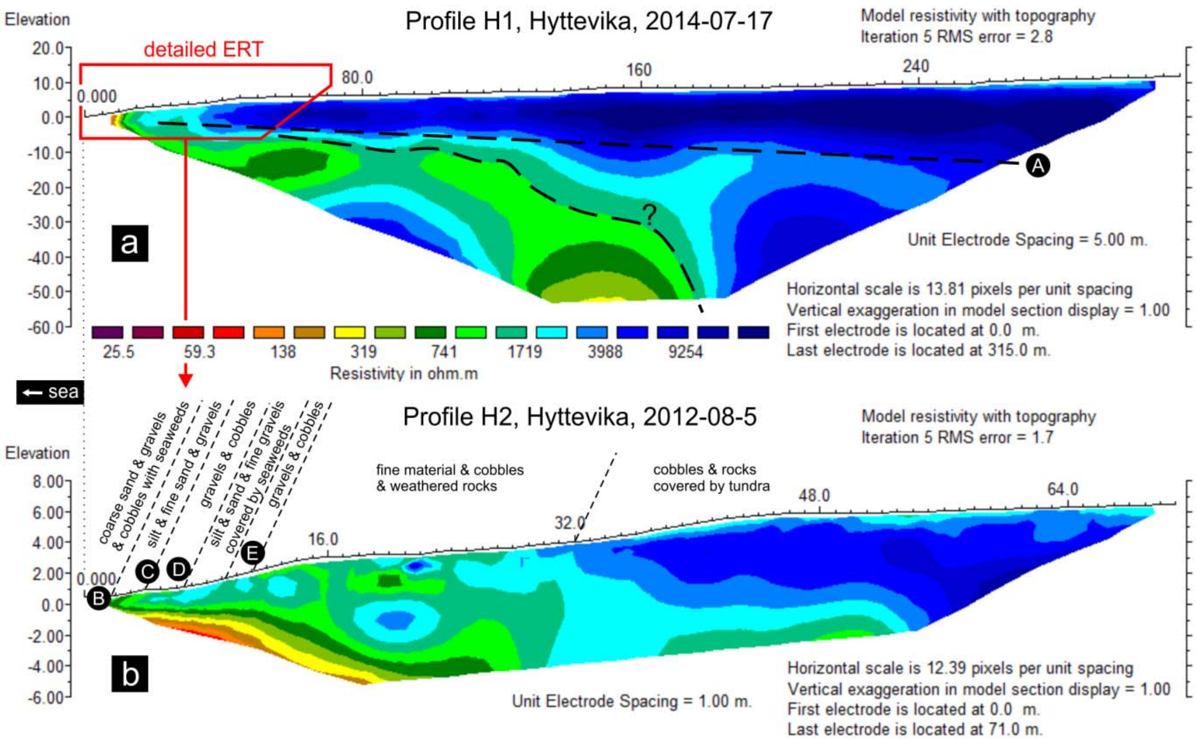

Fig. 9. a) Inversion results of electrical imaging in Hyttevika; b) more detailed ERt image of coastal zone. Legend: A –boundaries between permafrost and non-frozen ground below (permafrost base),. B – berm, C – storm ridge, D – swale, E – older storm ridge (abraded slope). The colour scale was unified for all resistivity models.

In Profile H2, carried out in August 2012 (Fig. 9b), the inland penetration of a wedge of high resistivity was clearly visible. Approximately 32 metres from the start of the profile (low-water mark) and before reaching the area covered by uplifted marine terrace (6–8 m a.s.l.), a noticeable resistivity change in the upper part of ground was detected. Almost on the entire length of the profile the formation of active layer with lower resistivity than in deeper parts of the profile was observed. The active layer thickness increased seaward from the section of the profile covered with uplifted marine landforms (terraces with beach ridges).

Veslebogen. The ERT measurements in Veslebogen indicated large differences between the inversion results of the profiles led across coastal zone in the sheltered embayment (Profile V1, Fig. 10 a)and in an exposed and relatively narrow (ca. 150 m wide) headland (Profile V2, Fig. 10 b). The low resistivity values interpreted as unfrozen rock were detected only along the edges of tomogram from seaside section of Profile 6 . In this place the electrical resistivity method with the available quantity of terminals for electrodes reached the limits of its usefulness. Coastal zone in Profile V1 contained frozen body of dozen of meters thick in the area up to 70 m from the shoreline, and up to 40 meters thick from 180 m inland.

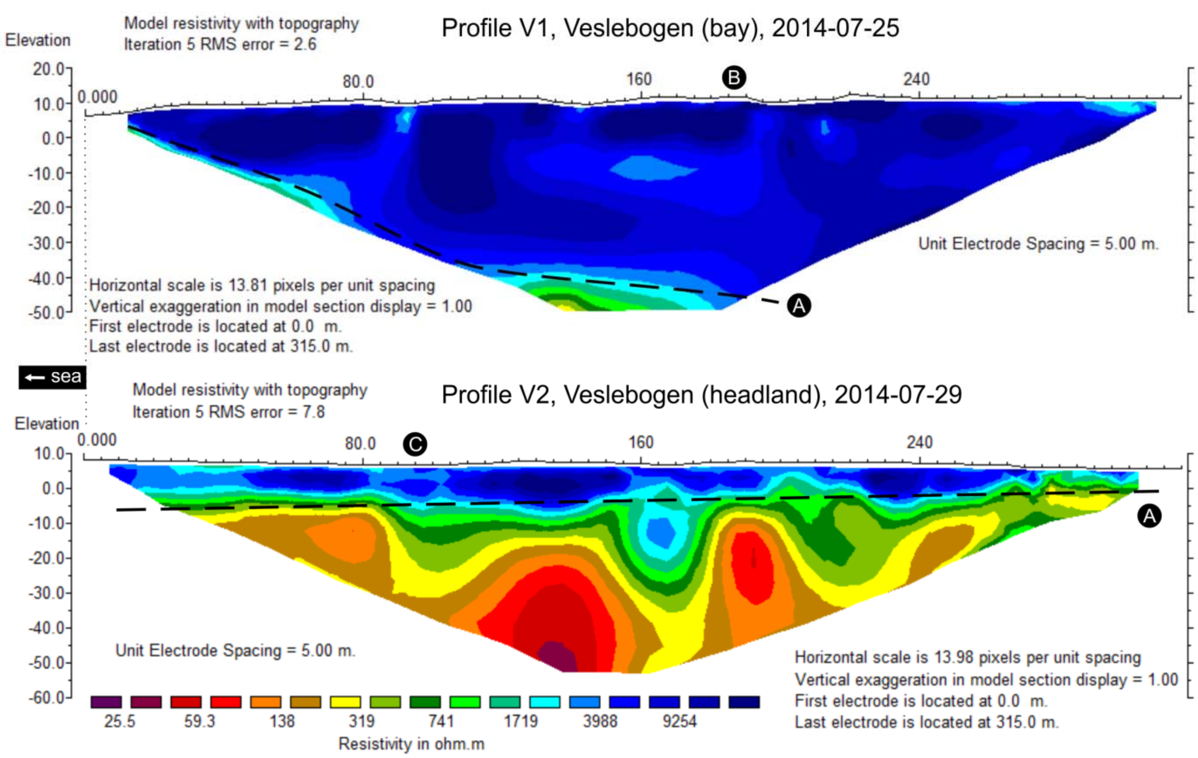

Fig. 10 Inversion results of electrical imaging in Veslebogen :a) sheltered embayment, b) headland exposed to the operation of waves and tides. Legend: A – presumed bounduary between permafrost and non-frozen ground below (permafrost base), B – solid rocks (paleoskiers), C – single frost crack. The colour scale was unified for all resistivity models.

The inversion results from the headland (Profile V2) were drastically different than in the embayment. High resistivity $\rho > 1$ kΩ m was characteristic only for the upper part of the profile, to the depth of 5–10 m, and were interpreted as a permafrost. The lithological boundary at ca. 2.5–3 m depth between marine gravels covering the top of headland and solid rock (Fig. 5d) was not distinguishable in terms of electrical resistivity. The lower parts of the profile showed a notably lower electrical resistivity ($\rho < 300$ Ω m) and may be interpreted as unfrozen solid rock. Such a situation may be associated with the exposure of the headland to the operation of waves and tides affecting physical and chemical properties of the rock.

Discussion

The ERT measurements and interpretation of the inversion models require few comments on the possible measuring and interpretation errors. Due to the time limit and safety reasons (wandering polar bears, damage of measuring cables by polar foxes and reindeers) the measurements were conducted only once and using only one method. The chosen measurement method (Wenner-Schlumberger) is relatively universal one in imaging horizontal and vertical structures, but could not provide deeper penetration, as in the Dipole-Dipole electrode array (Reynolds 2011). The received inversion models, though used to deduce on the ground thermal state, relate directly not to the temperature but apparent resistivity. In addition, their graphical representation is a result of interpolation, which largely depend on the distribution of points with extreme values. Therefore our interpretation of the inversion results, not supported with ground temperature monitoring, was based on the geoelectrical characteristics of rocks known from the literature (see Fig. 3). In our study we have also considered the results of previous works comparing the ground temperature data with the ERT data (e.g. Hayley et al. 2007, Overduin et al. 2012, You et al. 2013), with particular attention on reports from surveys across coastal and nearshore zones (e.g. Sellmann et al. 1988). Nevertheless, information from literature is not consistent, and difficulties in establishing a clear range of resistivity typical for the permafrost, result from many factors affecting the geoelectrical properties of the ground. For this reason, marking of the boundary between frozen and unfrozen grounds shown in Figures 8–10 was arbitrary. In case of Profiles S1 and H1 two alternative variants of a boundary have been suggested.

We took for granted that the ground electrical resistivity strongly depends on its thermal state (Rein et al. 2004, Halley et al. 2007). Field observations carried out by MacKay (1969) showed that the apparent resistivity of the rock mass increases together with temperature fall. MacKay's (1969) study also pointed to large resistivity differences (2–3 orders of magnitude) characterising surface sediments of Mackenzie River Delta. The resistivity of frozen gravel with sand was determined at 20–22 kΩ m, while unfrozen sand and gravel had resistivity at 0.015–0.080 kΩ m. The connections of resistivity changes depending on the ground thermal state were also proved by the Antarctic study by McGinnis et al. (1973) carried out over a wide range of negative . The authors demonstrated that the value of ρ = 1 kΩ m does not have to indicate rock freezing. McGinnis et al. (1973) paid attention on the issue of ground porosity and found out that at 0°C all saturated porous soils and rocks have resistivity lower than 700, whereas small nonporous rocks may have resistivity as great as 5 000.

Similar measurements carried out in 20–50 m deep boreholes in Qumahe in the east of the Tibetan Plateau indicated that frozen formations may have much lower resistivity, about ρ ≈180 Ω m (You et al. 2013). However, other permafrost resistivity measurements show quite contrasting situation. Larin et al. (1978) found out that in the Arctic islands and along (Siberian) Arctic coasts Quaternary sediments have resistivity 0.8–80 kΩ m and pre-Quaternary rocks 1–3 kΩ m, whereas subpermafrost and intrapermafrost horizons of the fresh and slightly saline water are characterised by resistivity of about 0.1 kΩ m. Similar measurements of electrical properties of frozen silt made by Arcone and Delaney (1988) showed that the ground resistivity values above ρ > 1 kΩ m generally indicate ice content higher than 40%.

The interpretation of received inversion results is facilitated by the fact that the subject of the research is ground with relatively high temperature, so called "warm permafrost" (Gregersen and Eidsmoen 1988). In Spitsbergen, the borehole temperature measurements demonstrated that at 30 m depths the permafrost temperatures are –3.0°C and –2.4°C at the mineralization of aquifers 34–44 $g \cdot l^{-1}$ (Oberman and Kakunov 1978). Similar calculations supported by the ground thermal measurements in Longyearbyen and Svea allowed Gregory and Eidsmoen (1988) to infer that along the southern and western coasts of Spitsbergen the mean ground temperature inside the in the shore is 1–2°C below zero, while further inland the surface temperature is above zero and permafrost conditions are present at few metres depths.

It is also difficult to clearly distinguish the differences in resistivity caused by the thermal state from the differences arising from the salinity of the coastal sediments. According to Gregersen et al. (1983) salty soils remain unfrozen even at –2 to –3°C. During the investigations of the phase composition of the water and structural properties of saline soils Tsytovich et al. (1978) noticed a shift of the phase transition from about –0.4 to –1.6°C (frozen) and –0.6 to –3.5°C (thawed) for soils with low salinity and from –1.2 to –21.8°C (frozen) and –4.9 to –41.0°C (thawed) for soils with high salinity.

Very low resistivity values observed during this study in the seaward part of the coastal zone (even ρ < 50 Ω m) indicate that this zone is unfrozen, at least in the subsurface layer of the intertidal zone. The lack of submarine permafrost in the coastal zone contradicts the first calculations of Werenskiold (1922), and is different from the conditions of the coastal zone in other parts of the Arctic, e.g. the Kara Sea (Rekant et al. 2005) or the Beaufort Sea (Hunter et al., 1988, Overduin et al. 2012). However, it is coherent with the views on the state of Svalbard coastal zone presented by Soloviev (1988) who stated that the seabed along the eastern coast of the Svalbard is devoid of permafrost. According to Soloviev (1988) the seabed along northern Spitsbergen and Franz Josef Land coasts remains mainly unfrozen, and seasonal freezing of sediments deposited at the bottom of the coastal waters starts around the southern tip of Novaya Zemlya (φ 70°N). The zone of the permanently frozen seabed extends approximately from the central part of Novaya Zemlya to the north-east (in the direction of Franz Josef Land).

Our results suggests that the thawed zone continues from the sea towards the land and continues under the permafrost body. The geometrical arrangement between bodies with different resistivity resembles the shape of the contact zone between seawater and freshwaters with different physical and chemical features observed on carbonate islands and coasts of Bahamas (Mylroie and Carew 2000, 2003). In the aforementioned example, in less mineralised freshwater karstic voids have developed. In case of our study site the permafrost body would correspond to the shape of freshwater lens which base was shaped in the zone of halocline (vertical salinity gradient within a body of water, where the fresh-water to salt-water boundary is sharp or in the mixing zone). The inversion results suggest that permafrost thickness in the coastal zone exposed to operation of waves and tides is very limited. A body of resistivity ρ > 1 kΩ m at the distance of 100 m from the shoreline is thinner than 10 m (except Profile V1 in sheltered embayment). Similar thawing of the ground under permafrost was previously observed in more inland areas and linked with the underground discharge of meltwaters from glaciers (e.g. Haldorsen et al. 1996, Booij et al. 1998, Haldorsen et al. 2010). However, the spatial variation of permafrost thickness was not the subject of those investigations, and in our opinion the established patterns of the water discharge under the permafrost were too simplified. For example, Haldorsen et al. (1996) showed permafrost in a schematic model of the subpermafrost groundwater system as a body of practically constant thickness of ca. 100 m across the entire coastal zone and ending in the seabed zone. Therefore, their general model contradicts our interpretation and do not fit into a well-known pattern, presented by Lachenbruch (1968) or Gold and Lachenbruch (1973), showing the effect of surface features on the distribution of permafrost in the continuous permafrost zone. It is noteworthy that smaller thickness of coastal permafrost was indicated by earlier investigations by Harada and Yoshikawa (1996, 1988). The electrical soundings with the Wenner electrode configuration in the Adventdalen delta (2 m a.s.l.) allowed them to define the permafrost thickness of 31.7 m.

To our knowledge the influence of the shape of the coast on permafrost thickness has not been studied. Our results show that on the contrary to sheltered embayments the operation of wave and tides on exposed parts of the coastal zone (headlands) results in a weaker development of permafrost. Perhaps this relationship was taken into account by Gregersen and Eidsmoen (1988), who included "shoreline topography" in the list of local factors controlling coastal permafrost properties. Variations in permafrost thawing conditions was previously studied along the shelf of Canadian Beaufort Sea. Hunter et al. (1988) showed that the summertime temperature configuration indicated a thin thaw zone above 0°C along the entire shelf section out to 800 m offshore. In the nearshore zone, at water depths less than 1 m, the thaw zone was less than 0.5 m thick. In deeper waters (>2 m), the thaw zone increased to 8 m thickness.

The resistivity models received from our study show that coastal permafrost is not homogenous. As presented on each of the tomograms, the permafrost body with the highest resistivity in the subsurface section of the ground is highly differentiated in terms of resistivity. This is particularly evident in profiles characterised by higher resolution (Profiles S2, S3, H2). The highest resistivities $\rho > 2$ kΩ m were marked just 10–20 meters from the shore. In Profile S3, the existence of several 'islands' of high resistivities along the distance of 100 m to the sea actually reminds discontinuous permafrost. However, we agree that without ground temperature measurements, such a conclusion may not be clearly verified, especially when we take into account that according to Brown et al. (1997) Svalbard lays in a zone of continuous permafrost (extent of 90–100%).

In each profile the active layer was characterised with reduced resistivity. Due to the limits of the ERT method (no registration of surface points) and applied electrode spacing, only the bottom part of the active layer was registered even in the profiles with higher resolution. In general active layer thawing from the ground was weaker under beach ridges and stronger in depressions filed with humid mires. Development of thicker active layer in Profile 3 than in Profile S2 may be associated with the timing of measurement. Profile S3 was carried out one month later than Profile S2 (August 2012 – July 2014). Second factor that may led to stronger thawing of active layer in 2012 were meteorological conditions during the spring period (see Fig. 6). In contrast to the spring 2014 the spring 2012 was devoid of thick snow cover which has a strong influence on active layer thawing (Harris et al. 2009). Although in 2012 the ground temperatures at 1m depth rose above 0°C earlier than in 2014 (6th of June 2012 – 19th of June 2014) in August 2014 the ground temperature was higher than in August 2012. On the 13th of August 2012 the ground temperature at 1m was 3.4°C, while on the 9th of August 2014 the temperature reached 4.8°C. Overall, the ERT image of the thawed ground generally confirmed the earlier near-surface observations on the state of permafrost in Hornsund region (Baranowski 1968, Jahn 1982, Grześ 1985, Chmal et al. 1988, Migała 1994, Dolnicki et al. 2013).

The repeated ERT measurements in 2012 and 2014 (Profiles S2 and S3) documented also resistivity changes in deeper ground sections. We have associated those changes with the impact of seawater temperature and salinity. Similar conclusion was presented by Molochushkin (1978) who discovered that even relatively cold (mean annual temperature 0.2–0.3°C) and slightly salty (20‰) seawater in the Laptev Sea accelerated the degradation of coastal permafrost. Several authors reported development of active layer in seabed sediments deposited along the coast of the Beaufort Sea (Mackay 1972, Hunter et al. 1988). The seasonal changes in the thermal state of submarine permafrost were associated with the impact of fluxes of warm freshwater from the Mackenzie River.

Our results confirmed that heat waves found in the winter 1986/1987 at the base of ground temperature monitoring boreholes may be caused by the influence of relatively warm and salty seawater on deeper ground sections. This study supplemented the observations by Baranowski (1968) by showing that the inland heat wave advancing the sea may affect the state of permafrost in solid rock. The dominant role on the variation in the resistivity values was played by a thermal factor. For instance, in Profile V2 strong freezing of geological formations covered up clear lithological boundaries in the received image. The obtained tomograms enabled analysis of spatial distribution of permafrost which is difficult to perform using individual boreholes. Borehole measurements have to include period of stabilization of permafrost temperature that at 1 m depth may last even up to 250 days (Gregersen and Eidsmoen 1988) leading to significant delay in obtaining reliable data on thermal state of the permafrost.

Conclusions

We draw seven conclusions from this study

1. Very low resistivity observed in the intertidal zone exclude existence of submarine permafrost at least in the nearshore zone.
2. Low ground resistivity continuing inland in deeper ground sections, impossible to explain with lithological changeability, provide evidence for strong influence of temperature and salinity of the sea on the permafrost base.
3. The shape of the permafrost base in close proximity to the sea reminds a wedge directed towards the shoreline.
4. Resistivity changes found in the same profile line at different times document the existence of the active layer existing from the side of the permafrost base.
5. The coastline shape configuration and exposure to wave and tidal action have a significant influence on the formation of deeper (>10 m) permafrost levels.

6. The effective interpretation of the active layer is possible with the use of small electrode spacing of 1 or 1.5 m during the ERT measurements.
7. The ERT measurements allowed monitoring of changes in spatial distribution of active layer and base of the coastal permafrost.

Acknowledgements

Paper is a contribution to the National Science Centre Project: '*Model of the interaction of paraglacial and periglacial processes in the coastal zone and their influence on the development of Arctic littoral relief*' award no. 2013/08/S/ST10/00585. Fieldwork was also supported by the Rector of the University of Wrocław and the Director of the Institute of Geography and Regional Development of the University of Wrocław. Assistance of Mr. Krzysztof Senderak during field work is gratefully acknowledged. Norwegian Polar Institute (Harald Aas) is thanked for providing a DEM of study area. Matt Strzelecki is supported by National Science Centre Postdoctoral Fellowship FUGA, the Ministry of Science and Higher Education Outstanding Young Scientists Scholarship, Foundation for Polish Science HOMING PLUS (grant no. 2013-8/12) and START grants.

References

Arcone, S.A., Delaney, A.J., 1988. Borehole investigations of the electrical properties of frozen silt. In: Senneset, K. (Ed.), Permafrost. Fifth International Conference. August 2–5, Proceedings Volume 2, Tapir Pub., Trondheim, Norway, pp. 910–915.

Baranowski, S., 1968. Thermic conditions of the periglacial tundra in SW Spitsbergen. Acta Universitas Wratislaviensis 68, Studia geograficzne X (in Polish with Eng. abstract), 74 p. and also translated and published in 1971 for the U.S. Dept. of Commerce Environmental Science Services Administration and the National Science Foundation, Washington, D.C. by the Scientific Publications Foreign Cooperation Center of the Central Institute for Scientific, Technical and Economic Information in Warsaw.

Booij, M., Leijnse, A., Haldorsen, S., Heim, M., Rueslåtten, H., 1998. Subpermafrost ground modeling in Ny-Ålesund, Svalbard. Nordic Hydrology 29(4/5), 358–396.

Brown, J., Ferrians, O., Heginbottom, J.A. and Melnikov, E.S. 1997. Circum-arctic map of permafrost and ground-ice conditions. 1:10,000,000 Map CP-45. Circum-Pacific map series, USGS.

Byun, Y.-H., Yoon, H.-K., Kim, Y.S., Hong, S.S., Lee, J.-S., 2014. Active layer characterization by instrumented dynamic cone penetrometer in Ny-Alesund, Svalbard. Cold Regions Science and Technology 104–105, 45–53, Chmal H. 1987. Pleistocene sea level changes and glacial history of the Hornsund area, Svalbard. Polar Research 5, 269–270, doi:10.1016/j.coldregions.2014.04.003

Chmal, H., Klementowski, J., Migała, K., 1988. Thermal currents of active layer in Hornsund area. In: Senneset, K. (Ed.), Permafrost. Fifth International Conference. August 2–5, Proceedings Volume 1, Tapir Pub., Trondheim, Norway, pp. 44–49.

Christiansen, H.H., Etzelmüller, B., Isaksen, K., Juliussen, H., Farbrot, H., Humlum, O., Johansson, M., Ingeman-Nielsen, T., Kristensen, L., Hjort, J., Holmlund, P., Sannel, A. B. K., Sigsgaard, C., Akerman, H. J., Foged, N., Blikra, L. H., Pernosky, M. A., and Odegard, R. S.: The thermal state of permafrost in the Nordic Area during the International Polar Year 2007–2009. Permafrost and Periglacial Processes 21, 156–181, doi:10.1002/P pp.687, 2010

Christiansen, H.H., Humlum, O., 2008. Interannual variations in active layer thickness in Svalbard. In: Kane, D.L., Hinkel K.M. (Eds), Proceedings Ninth International Conference on Permafrost, June 29–July 3, Fairbanks Alaska, Vol. 1. Institute of Northern Engineering, University of Alaska, Fairbanks, pp. 257–262.

Cox J.C., Monde M.C., 1985. *Wave erosion of an unprotected frozen gravel berm.* Arctec Engineering Inc., 43 p.

Czerny, J., Kieres,. A., Manecki, M., Rajchel, J., 1992. Geological Map of the SW Part of Wedel Jarlsberg Land Spitsbergen, 1:25 000. Institute of Geology and Mineral Deposits, Univ. of Mining and Metallurgy, Cracow.

Dobiński, W., 2011. Permafrost. Earth-Science Reviews 108, 158–169.

Dolnicki, P., Grabiec, M., Puczko, D., Gawor, Ł., Budzik, T., Klementowski, J., 2013. Variability of temperature and thickness of permafrost active layer at coastal sites of Svalbard. Polish Polar Research 34(4), 353–374.

Etzelmüller, B., Schuler, T.V., Isaksen, K., Christiansen, H.H., Farbrot H., Benestad, R., 2011. Modeling the temperature evolution of Svalbard permafrost during the 20th and 21st century. The Cryosphere 5, 67–79. doi:10.5194/tc-5-67-2011

Gerland, S., Hall, R., 2006. Variability of fast-ice thickness in Spitsbergen fjords. Annals of Glaciology 44, 231–239.

Gregersen, O., Eidsmoen, T., 1988, Permafrost conditions in the shore area at Svalbard. In: Senneset, K. (Ed.), Permafrost. Fifth International Conference. August 2–5, Proceedings Volume 2, Tapir Pub., Trondheim, Norway, pp. 933–936.

Gregersen, O., Phukan, A., Johansen, T., 1983. Engineering properties and foundation design alternatives in marine Svea clay, Svalbard. International Conference on Permafrost 4, Fairbanks, Alaska 1983. Proceedings, pp. 384–388. Also publ. in: Norwegian Geotechnical Institute, Oslo, Publ. No. 159, 1985.

Gold, L.W., Lachenbruch, A.H., 1973. Thermal conditions in permafrost – a review of North American literature. In: Permafrost Second International Conference, 13–28 July 1973, Yakutsk, U.S.R.R., North American Contribution, Arlis, National Academy of Sciences, Washington, pp. 3–25.

Haldorsen, S., Heim, M., Lauritzen, S.-E., 1996. Subpermafrost Groundwater. Western Svalbard. Nordic Hydrology 27, 57–68.

Haldorsen, S., Heim, M., Dale, B., Landvik, J.Y., van der Ploeg, M., Leijnse, A., Salvigsen, O., Hagen, J.O., Banks, D., 2010. Sensitivity to long-term climate change of subpermafrost groundwater systems in Svalbard. Quaternary Research 73, 393–402, doi:10.1016/j.yqres.2009.11.002

Halley, K., Bentley, L.R., Gharibi, M., Nightingale, M., 2007. Low temperature dependence of electrical resistivity: Implications for near surface geophysical monitoring. Geophysical Research Letters 34, L18402, doi:10.1029/2007GL031124

Harada, K., Yoshikawa, K., 1996. Permafrost age and thickness near Adventfjorden, Spitsbergen. Permafrost – Seventh International Conference (Proceedings), Yellowknife (Canada), Collection Nordicana 55, pp. 427–431.

Harada, K., Yoshikawa, K., 1998. Permafrost age and thickness at Moskuslagoon, Spitsbergen. Polar Geography 20(4), 267–281, doi: 10.1080/10889379609377607

Harris, C., Arenson, L.U., Christiansen, H.H., Etzelmüller, B., Frauenfelder, R., Gruber, S., Haeberli, W., Hauck, C., Hölzle, M., Humlum, O., Isaksen, K., Kääb, A., Kern-Lütschg, M.A., Lehning, M. Matsuoka, N., Murton, J. B., Nötzli, J., Phillips, M., Ross, N., Seppälä, M., Springman, S. M., Mühll, D.V., 2009. Permafrost and climate in Europe: Monitoring and modelling thermal, geomorphological and geotechnical responses. Earth-Science Reviews 92, 117–171, doi 10.1016/j.earscirev.2008.12.002

Hauck, C., 2002. Frozen ground monitoring using DC resistivity tomography. Geophysical Research Letters 29(21), 2016, doi:10.1029/2002GL014995

Hauck, C., 2013. New Concepts in Geophysical Surveying and Data Interpretation for Permafrost Terrain. Permafrost and Periglacial Processes 24, 131–137, doi: 10.1002/ppp.1774

Hilbich, C., Marescot, L., Hauck, C., Loke, M.H., Mäusbacher, R., 2009. Applicability of Electrical Resistivity Tomography Monitoring to Coarse Blocky and Ice-rich Permafrost Landforms. Permafrost and Periglacial Processes 20(3), 269–284, doi 10.1002/ppp.652

Humlum, O., Instanes, A., Sollid, J.L., 2003. Permafrost in Svalbard: a review of research history, climatic background and engineering challenges. *Polar Research* 22(2), 191–215, doi 10.1111/j.1751-8369.2003.tb00107.x

Hunter, J.A., Mac Aulay, H.A., Pullan, S.E., Gagné, R.M., Burns, R.A., Good, R.L., 1988, Thermal evidence for an active layer on the seabottom of the Canadian Beaufort Sea shelf. In: Senneset, K. (Ed.), Permafrost. Fifth International Conference. August 2–5, Proceedings Volume 2, Tapir Pub., Trondheim, Norway, pp. 949–954.

Isaksen, K., Benestad, R.E., Harris, C., Sollid, J.L., 2007. Recent extreme near-surface permafrost temperatures on Svalbard in relation to future climate scenarios. Geophysical Research Letters 34, L17502, doi:10.1029/2007GL031002

Isaksen, K., Holmlund, P., Sollid, J.L., Harris, C., 2001. Three Deep Alpine-Permafrost Boreholes in Svalbard and Scandinavia. Permafrost and Periglacial Processes 12, 13–25, doi: 10.1002/ppp 380

Ishikawa, M., 2004, Application of DC resistivity imaging to frozen ground investigations. Journal of the Japanese Society of Snow and Ice 66(2), 177–186, doi.org/10.5331/seppyo.66.177

Jahn, A., 1959. Postglacial development of Spitsbergen shores (in Polish). *Czasopismo Geograficzne*, 30, 245–262.

Jahn, A., 1968. Raised shore lines and terraces at Hornsund, and postglacial vertical movements on Spitsbergen. In: Birkenmajer, K. (Ed.), Polish Spitsbergen Expeditions 1957–1960, Polish Academy of Science, III I.G.Y./I.G.C. Committee, Warszawa, pp. 173–176.

Jahn, A., 1982. Soil thawing and active layer of permafrost in Spitsbergen. Acta Universitatis Wratislaviensis 525, Spitsbergen Expeditions IV, pp. 57–75.

Kabała, C., Zapart, J., 2009. Recent, relic and buried soils in the forefield of Werenskiold Glacier, SW Spitsbergen. Polish Polar Research 30(2), 161–178.

Karczewski, A., Andrzejewski, L., Chmal, H., Jania, J., Kłysz, P., Kostrzewski, A., Lindner, L., Marks, L., Pękala, K., Pulina, M., Rudowski, S. Stankowski, W., Szczypek, T., Wiśniewski E., 1990. Hornsund, Spitsbergen Geomorphology, 1:75 000 (with commentary to the map by Karczewski, A.). Polish Academy of Sciences, Silesian University, Katowice.

Kearey, P., Brooks, M., Hill, I., 2002. Electrical surveying. In: An Introduction to Geophysical Exploration 3rd Edition. Blackwell Science.

Kienast, F., Wetterich, S., Kuzmina, S., Schirrmeister, L., Andreev, A.,Tarasov, P., Nazarova, L., Kossler, A., Frolova, L., Kunitsky, V., 2011. Paleontological records indicate the occurrence of open woodlands in a dry inland climate at the present-day Arctic coast in western Beringia during the Last Interglacial. *Quaternary Science Reviews* 30, 2134-2159.

King, L., Seppälä, M., 1987. Permafrost thickness and distribution in Finnish Lapland – results of geoelectrical soundings. Polarforschung 57(3), 127–147.

Kneisel, C., 2010. Frozen ground conditions in a subarctic mountain environment, Northern Sweden. Geomorphology 118, 80–92, doi 10.1016/j.geomorph.2009.12.010

Kneisel, C., Hauck, C., 2008. Electrical methods. In: C. Hauck & C. Kneisel (Eds.), Applied Geophysics in Periglacial Environments. Cambridge Univ. Press., pp. 3–27.

Kneisel, C., Hauck, C., Fortier, R., Moorman, B. 2008. Advances in geophysical methods for permafrost investigations. Permafrost and Periglacial Processes 19, 157–178, doi 10.1002/ppp.616

Kneisel, C., Emmert, A., Kästl, J., 2014. Application of 3D electrical resistivity imaging for mapping frozen ground conditions exemplified by three case studies. Geomorphology, doi: 10.1016/j.geomorph.2013.12.022.

Krautblatter, M., Hauck, C., 2007. Electrical resistivity tomography monitoring of permafrost in solid rock walls. Journal of Geophysical Research: Earth Surface 112, F2, 2156–2202, doi 10.1029/2006JF000546

Lachenbruch, A.H., 1968. Permafrost. In: Fairbridge, R.W. (Ed.), The encyclopedia of geomorphology. New York, Reinhold Pub. Corp., pp. 833–839.

Larin, S.M., Marov, G.P., Kholmyanskiy, M.A., Neizvestnov, Ya.V., 1978. Certain types of geoelectric sections of the negative temperature belt in the arctic and subarctic connection with exploration for subpermafrost. In: Sanger, F.J, Hyde, P.J. (Eds), Permafrost Second International Conference, 13–28 July 1973, Yakutsk, U.S.R.R., USRR Contribution, National Academy of Sciences, Washington, pp. 428–430.

Leszkiewicz, J., Caputa, Z., 2004. The thermal condition of the active layer in the permafrost at Horsund, Spitsbergen. Polish Polar Research 25(3–4), 223–239.

Lewkowicz, A.G., Etzelmüller, B., Smith, S.L., 2011. Characteristics of discontinuous permafrost based on ground temperature measurements and electrical resistivity tomography, Southern Yukon, Canada. Permafrost and Periglacial Processes 22 (4), 320–342, doi 10.1002/ppp.703

Liestøl, O., 1976. Pingos, springs, and permafrost in Spitsbergen. Nor. Polarinst. Årb. 1975, 7–29.

Loke, M.H., 2000. Electrical imaging syrveys for environmental and engineering studies. A practical guide to 2-D and 3-D surveys. Geotomo, Malaysia.

Loke, M.H., 2013. *Manual for RES3DINV. Rapid 3-D Resistivity & IP inversion using the least-squares method (For 3-D surveys using the pole-pole, pole-dipole, dipole-dipole, rectangular, Wenner, Wenner-Schlumberger and non-conventional arrays). On land, aquatic and cross-borehole surveys*. Geoelectrical Imaging 2-D & 3-D. Geotomo, Malaysia.

Loke, M.H., Chambers, J.E., Rucker, D.F., Kuras, O., Wilkinson, P.B., 2013. Recent developments in the direct current geoelectrical imaging method. Journal of Applied Geophysics 95, 135–156, doi 10.1016/j.jappgeo.2013.02.017

Łupikasza, E., 2013. Atmospheric precipitation. In: A.A. Marsz & A. Styszyńska (Eds), *Climate and Climate change at Hornsund, Svalbard*. Gdynia Maritime Univ., pp. 199–211.

Kępski, D., Górski, Z., Benedyk, M., Szumny, M., Wawrzyniak, T. (Eds), 2013. Meteorological bulletin. Spitsbergen-Hornsund. Summary of the year 2013. Polish Polar Station, Institute of Geophysics, Polish Academy of Sciences.

MacKay, D.K., 1969. Electrical resistivity measurements in frozen ground, Mackenzie Delta area, Northwest Territories. Association Internationale d'Hydrologie Scientifique, Actes du Colloque de Becarest, Reprint Ser. 82, Department of Energy, Mines and Resources, Inland Waters Branch, Ceuterick, Belgium, pp. 363–375.

Mackay, J.R., 1972. Offshore permafrost and ground ice, Southern Beaufort Sea, Canada. Canadian Journal of Earth Sciences 9(11), 1550–1561.

Marsz, A.A., 2013a, Air temperature. In: A.A. Marsz & A. Styszyńska (Eds), *Climate and Climate change at Hornsund, Svalbard*. Gdynia Maritime Univ., pp. 145–187.

Marsz, A.A., 2013b, Humidity. In: A.A. Marsz & A. Styszyńska (Eds), *Climate and Climate change at Hornsund, Svalbard*. Gdynia Maritime Univ., pp. 189–198.

McCann, S.B., Hannell, F.G., 1971. Depth of the "frost table" on Arctic beaches, Cornwallis alld Devon Islands, N. W. T., Canada. *Joumal of Glaciology* 10, 155-158.

McGinnis, L.D., Nakao, K., Clark, C.C., 1973, Geophysical identification of frozen and unfrozen ground, Antarctica. In: Permafrost Second International Conference, 13–28 July 1973, Yakutsk, U.S.R.R., North American Contribution, Arlis, National Academy of Sciences, Washington, pp. 3–25.

Migała, K., Wojtuń, B., Szymański, W., Muskała P., 2014. Soil moisture and temperature variation under different types of tundra vegetation during the growing season: A case study from the Fuglebekken catchment, SW Spitsbergen. Catena 116, 10–18, doi 10.1016/j.catena.2013.12.007

Migoń, P., 1997. Post-emergence modification of marine cliffs and associated shore platforms in a periglacial environment, SW Spitzbergen: implications for the efficacy of cryoplanation processes. Quaternary Newsletter 81, 9–17.

Milsom, J., 2003. Resistivity methods. In: Field Geophysics 3rd Edition. Wiley, Chichester. 97–116.

Molochushkin, E.N., 1987. The effect of thermal abrasion on the temperature of the permafrost in the coastal zone of the Laptev Sea. In: Sanger, F.J, Hyde, P.J. (Eds), Permafrost Second International Conference, 13–28 July 1973, Yakutsk, U.S.R.R., USRR Contribution, National Academy of Sciences, Washington, pp. 90–93.

Mylroie, J.E., Carew, J.L., 2000. Speleogenesis in coastal and oceanic settings. In: Klimchouk, A.B., Ford, D.C., Palmer, A.N., Dreybrodt W. (Eds.), Speleogenesis, evolution of karst aquifers. National Speleological Society, pp. 226–233.

Mylroie, J.E., Carew, J.L., 2003. Karst development on carbonate islands. Speleogenesis and Evolution of Karst Aquifers 1(2), 1–21.

Niedźwiedź, T., Styszyńska, A., 2013. Snow cover at the Hornsund Station. In: A.A. Marsz & A. Styszyńska (Eds), *Climate and Climate change at Hornsund, Svalbard*. Gdynia Maritime Univ., pp. 367–372.

Oberman, N.G., Kakunov, B.B., 1978. Determination of the thickness of permafrost on the Arctic coast. In: Sanger, F.J, Hyde, P.J. (Eds), Permafrost Second

International Conference, 13–28 July 1973, Yakutsk, U.S.R.R., USRR Contribution, National Academy of Sciences, Washington, pp. 143–147.

Overduin, P.P., Westermann, S., Yoshikawa, K., Haberlau, T., Romanovsky, V., Wetterich, S., 2012. Geoelectric observations of the degradation of nearshore submarine permafrost at Barrow (Alaskan Beaufort Sea). Journal of Geophysical Research: Earth Surface 117, F2, 1–9, doi 10.1029/2011JF002088

Overduin, P. P.; Strzelecki, M. C.; Grigoriev, M. N.; Couture, N.; Lantuit, H.; St-Hilaire-Gravel, D.; Günther, F. and Wetterich, S., 2014. Coastal changes in the Arctic. In Martini, I. P. and Wanless, H. R., eds. Sedimentary coastal zones from high to low latitudes: similarities and differences. London, Geological Society, Special Publication 388: 103–130.

Péwé, T., 1979. Svalbard geology and permafrost. Natl. Sci. Found. Trip rep. 1979.

Ploeg, M. J. van der, Haldorsen, S., Leijnse, A., Heim, M., 2012. Subpermafrost groundwater systems: Dealing with virtual reality while having virtually no data. Journal of Hydrology 475, 42–52, doi:10.1016/j.jhydrol.2012.08.046

Rachlewicz, G., Szczuciński, W., 2008. Changes in thermal structure of permafrost active layer in dry polar climate, Petuniabukta, Svalbard. Polish Polar Research 29(3), 261–278.

Rein, A., Hoffmann, R., Dietrich, P., 2004. Influence of natural time- dependent variations of electrical conductivity on DC resistivity measurements. Journal of Hydrology 285(1–4), 215–232.

Rekant, P., Cherkashev, G., Vanstein, B., Krinitsky P., 2004. Submarine permafrost in the nearshore zone of the southwestern Kara Sea. Geo-Marine Letters 25, 2–3, 183–189. doi 10.1007/s00367-004-0199-5

Reynolds, J.M., 2011. Electrical Resistivity Methods. In: An Introduction to Applied and Environmental Geophysics. 2nd Ed., Wiley, Chichester, pp. 289–372.

Rodzik, J., Wiktorowicz, S., 1995. Shore ice of Hornsund fiord in the area of the Polish Polar Station in Spitsbergen during the 1992/93 winter. In: Wyprawy Geograficzne na Spitsbergen UMCS, Lublin, pp. 191–198.

Samouëlian, A., Cousina, I., Tabbagh, A., Bruandd, A., Richard, G., 2005. Electrical resistivity survey in soil science: a review. Soil and Tillage Research 83, 173–193, doi 10.1016/j.still.2004.10.004

Schrott, L., Sass, S., 2008. Application of field geophysics in geomorphology: Advances and limitations exemplified by case studies. Geomorphology 93, 55–73. doi; 10.1016/j.geomorph.2006.12.024

Seguin, M.K., Gahe, E., Allard, M., Ben-Mikoud, K., 1988. Permafrost geophysical investigation at the new airport site of Kangiqsualujjuaq, Northern Quebec, Canada. In: Senneset, K. (Ed.), Permafrost. Fifth International Conference. August 2–5, Proceedings Volume 2, Tapir Pub., Trondheim, Norway, pp. 980–987.

Schirrmeister, L., Grosse, G., Kunitsky, V., Fuchs, M., Krbetschek, M., Andreev, A., Herzschuh, U., Babyi, O., Siegert, C., Meyer, H., Derevyagin, A., Wetterich, S., 2010. The mystery of Bunge Land (New Siberian Archipelago): implications for its formation based on palaeoenvironmental records, geomorphology, and remote sensing. *Quaternary Science Reviews* 29, 3598-3614.

Sellmann, P.V., Delaney, A.J., Arcone, S.A., 1988. D.C. resistivity along coast at Prudhoe Bay, Alaska. In: Senneset, K. (Ed.), Permafrost. Fifth International Conference. August 2–5, Proceedings Volume 2, Tapir Pub., Trondheim, Norway, pp. 988–993.

Soloviev, W. A., 1988, Barentsevomorski schelf. In: Ershov E.D. (Ed.), Geokriologia SSSR. Evropeiskaya chast SSSR (in Russian). Nedra, Moscow, pp. 259–261.

Stenzel, P., Szymanko, J., 1973. Geophysical methods in hydrogeological and engineering-geological studies (in Polish). Geological Publ., Warsaw.

Swerpel, S., 1982. Hydrological investigations of the coastal waters in the Hornsund Fiord in the summer of 1975. Acta Universitatis Wratislaviensis 525, Results of Investigations of the Polish Scientific Spitsbergen Expeditions IV, 235–253.

Swerpel, S., 1985. The Hornsund Fiord: Water Masses. Polish Polar Research 6(4), 475–496.

Szymański, W., Skiba, S., Wojtuń, B., 2013. Distribution, genesis, and properties of Arctic soils: a case study from the Fuglebekken catchment, Spitsbergen. Polish Polar Research 34 (3), 289–304.

Telford, W.M., Geldart, L.P., Sheriff, R.E. 1990. Applied Geophysics 2nd Edition. Cambridge Univ. Press.

Trenhaile, A.S., 1997. *Coastal Dynamics and Landforms.* Oxford University Press, Oxford UK. 366pp.

Tsytovich, N.A., Kronik, Ya.A, Markin, K.F., Aksenov, V.I., Samuel'son, M.V., 1978. Physical and mechanical properties of saline soils. In: Sanger, F.J, Hyde, P.J. (Eds), Permafrost Second International Conference, 13–28 July 1973, Yakutsk, U.S.R.R., USRR Contribution, National Academy of Sciences, Washington, pp. 238–247.

Urbański, J., Neugebauer, E., Spajcer, R., Falkowska, L., 1980. Physico-chemical characteristic of the waters of Hornsund Fjord on south-west Spitsbergen (Svalbard Archipelago) in the summer season 1979. Polish Polar Research 1(4), 43–52.

Watanabe, T., Matsuoka, N., Christiansen, H.H., 2012. Mudboil and ice-wedge dynamics investigated by electrical resistivity tomography, ground temperatures and surface movements in Svalbard. Geografiska Annaler A 94 (4), 445–457, doi 10.1111/j.1468-0459.2012.00470.x

Werenskiold, W., 1922. Frozen earth in Spitsbergen. Geofysiske publikationer II, 10, pp. 3–10.

Węsławski, J.M., Zajączkowski, M., Kwaśniewski, S., Jezierski, J., Moskal, W., 1988. Seasonality in an Arctic fjors ecosystem: Hornsund, Spitsbergen. Polar Research 6, 185–189.

Westermann, S., Langer, M., Boike, J., 2011. Spatial and temporal variations of summer surface temperatures of high-arctic tundra on Svalbard — Implications for MODIS LST based permafrost monitoring. Remote Sensing of Environment 115(3), 908922, doi:10.1016/j.rse.2007.03.025

Wetterich, S., Kuzmina, S., Andreev, A., Kienast, F., Meyer, H., Schirrmeister, L., Kuznetsova, T., Sierralta, M., 2008. Palaeoenvironmental dynamics inferred from Late Quaternary permafrost deposits on Kurungnakh Island, Lena Delta, Northeast Siberia, Russia. *Quaternary Science Reviews* 27, 1523–1540.

Van Dam, R.L., 2012. Landform characterization using geophysics—Recent advances, applications, and emerging tools. Geomorphology 137, 57–73, doi 10.1016/j.geomorph.2010.09.005

Yoshikawa, K., Leuschen, C., Ikeda,A., Harada, K., Gogineni, P., Hoekstra, P., Hinzman L., Sawada, Y., Matsuoka, N., 2006. Comparison of geophysical investigations for detection of massive ground ice (pingo ice), Journal of Geophysical Research 111, E06S19, doi:10.1029/2005JE002573

You, Y., Yu, Q., Pan, X., Wang, X., Guo, L., 2013. Application of electrical resistivity tomography in investigating depth of permafrost base and permafrost structure in Tibetan Plateau. Cold Regions Science and Technology 87, 19–26, doi:10.1016/j.coldregions.2012.11.004.

Zajączkowski, M, Szczuciński, W., Plessen, B., Jernas, P., 2010. Benthic foraminifera in Hornsund, Svalbard: Implications for paleoenvironmental reconstructions. Polish Polar Research 31(4), 349–375, doi 10.2478/v10183-010-0010-4

Zwoliński, Z., Giżejewski, J.,Karczewski, A., Kasprzak, M., Lankauf, K.R., Migoń, P., Pękala, K., Repelewska-Pękalowa, J., Rachlewicz, G., Sobota, I., Stankowski, W., Zagórski, P., 2013, Geomorphological settings of Polish research areas on Spitsbergen. Landform Analysis 22, 125–143 doi: http://dx.doi.org/10.12657/landfana.022.011